

Temperature and equivalent temperature over the United States (1979–2005)

Souleymane Fall,^a Noah S. Diffenbaugh,^{a,b,c} Dev Niyogi,^{a,d,*} Roger A. Pielke Sr^e
and Gilbert Rochon^f

^a Department of Earth and Atmospheric Sciences, Purdue University, West Lafayette IN, USA

^b Purdue Climate Change Research Center, Purdue University, West Lafayette IN, USA

^c Department of Environmental Earth System Science and Woods Institute for the Environment, Stanford University, Stanford CA, USA

^d Department of Agronomy, Purdue University, West Lafayette IN, USA

^e CIRES and ATOC, University of Colorado, Boulder CO, USA

^f Purdue Terrestrial Observatory, Rosen Center for Advanced Computing, Purdue University, West Lafayette IN, USA

ABSTRACT: Temperature (T) and equivalent temperature (T_E) trends over the United States from 1979 to 2005 and their correlation to land cover types are investigated using National Centers for Environmental Prediction North American Regional Reanalysis data, the Advanced Very High Resolution Radiometer (AVHRR) land use/cover classification, the National Land Cover Database (NLCD) 1992–2001 Retrofit Land Cover Change and the Normalised Difference Vegetation Index (NDVI) derived from AVHRR. Even though most of the magnitude of T_E is explained by T , the moisture component induces larger trends and variability of T_E relative to T . The contrast between pronounced temporal and spatial differences between T and T_E at the near-surface level (2 m) and minor-to-no differences at 300–200 mb is a consistent pattern. This study therefore demonstrates that in addition to temperature, atmospheric heat content may help to quantify the differences between surface and tropospheric heating trends, and hence the impact of land cover types on the surface temperature changes. Correlations of T and T_E with NDVI reveal that T_E shows a stronger relationship to vegetation cover than T , especially during the growing season, with values that are significantly different and of opposite signs (-0.31 for T vs NDVI; 0.49 for T_E vs NDVI). Our results suggest that land cover types influence both moisture availability and temperature in the lower atmosphere and that T_E is larger in areas with higher physical evaporation and transpiration rates. As a result, T_E can be used as an additional metric for analysing near-surface heating trends with respect to land cover types. Moreover, T_E can be tested as a complementary variable for assessing the impact of land surface and boundary layer processes in re-analysis and weather/climate model studies. Copyright © 2010 Royal Meteorological Society

KEY WORDS temperature; equivalent temperature; heat content; NARR; AVHRR; NLCD; NDVI

Received 1 March 2009; Revised 11 November 2009; Accepted 28 December 2009

1. Introduction

Temperature variability and trends have been extensively investigated. Results from the huge body of studies indicate that significant warming took place over the last century (e.g. Jones *et al.*, 1986; Vinnikov *et al.*, 1990; Crowley and Lowery, 2000; IPCC, 2001, 2007; Mann and Jones, 2003; Soon *et al.*, 2004; Moberg *et al.*, 2005). Furthermore, climate model experiments and multiple observational datasets suggest that the warming observed in the ocean, at the surface and in the troposphere is consistent with anthropogenic greenhouse forcing of the climate system (Mears and Wentz, 2005; Barnett *et al.*, 2005a, 2005b; Santer *et al.*, 2005; Sherwood *et al.*, 2005; IPCC, 2007; Santer *et al.*, 2008).

Recent study also shows that atmospheric moisture content has increased in the past decades (Wentz and Schabel, 2000; Held and Soden, 2006; Santer *et al.*, 2007; Wentz *et al.*, 2007). Although positive trends in moisture content are consistent with positive trends in temperature, relatively few studies have focused on a simultaneous analysis that integrates temperature and moisture. Steadman (1979, 1984) derived a scale of apparent temperature, which expresses the combined effects of air temperature, vapour pressure, wind and solar radiation. Using observed temperature and humidity datasets over the 1961–1995 period, Gaffen and Ross (1999) found upward trends in apparent temperature over the United States. More recent studies focus on moist enthalpy (or, alternatively, equivalent temperature), which combines both air temperature and humidity in a single variable, to assess surface heating trends. Results from such studies suggest that the utilisation of temperature as a monitor of climate change may not provide a complete evaluation of the heat storage changes to the earth system (Pielke,

* Correspondence to: Dev Niyogi, Department of Agronomy and Department of Earth and Atmospheric Sciences, Indiana State Climate Office, Purdue University, West Lafayette, IN 47907, USA.
E-mail: climate@purdue.edu

2003), and that temperature, by itself, is an incomplete characterisation of surface air heat content (Pielke *et al.*, 2004; Davey *et al.*, 2006).

At a global scale, Ribera *et al.* (2004) used the NCEP/NCAR re-analysis temperature to study the relationships between equivalent temperature and modes of climate variability. The expression for moist enthalpy (Pielke *et al.*, 2004) is

$$H = C_p T + L_v q \quad (1)$$

where C_p is the specific heat of air at constant pressure, T is the air temperature, L_v is the latent heat of vapourisation and q is the specific humidity. Following the Priestley–Taylor method, L_v (J/kg) is estimated with the temperature function:

$$L_v = 2.5 - 0.0022 \times T \quad (2)$$

Such an estimate allows accounting for the variation of L_v with temperature, instead of assigning its approximate value at 30°C that has been used in previous studies. H is in units of Joule and must be scaled into degree units in order to obtain equivalent temperature for easy comparison to air temperature

$$T_E = H/C_p \quad (3)$$

Equation (3) can be also written as

$$T_E = T + \frac{L_v q}{C_p} \quad (4)$$

where L_v is in units of Joules per kilogram and C_p is in units of Joules per kilogram per degree K. As q is dimensionless (i.e. kg per kg), the ratio has units of degree K.

The motivation for the current study is to explore atmospheric heating as reflected in changes in both temperature and moisture. We focus on heating trends over the United States by comparing air temperature (T) and equivalent temperature (T_E) for different time scales, at near-surface (2 m) and standard pressure levels (up to 200 mb). In addition, because land use/cover change can affect the heat and moisture budgets at the surface (e.g. changes in transpiration from vegetation and evaporation from the surface hydrology), we relate both T and T_E to the normalised difference vegetation index (NDVI) and land use/cover to analyse their relationship with vegetation characteristics.

We describe the data and methods used in this study in Section 2. The results are presented in Section 3, followed by concluding remarks in Section 4.

2. Data and methods

Monthly T and specific humidity (q) at 2 m, 850 mb, 700 mb, 500 mb, 300 mb and 200 mb for the 1979–2005

period were obtained from the National Centers for Environmental Prediction (NCEP) North American Regional Reanalysis (NARR). NARR has been developed as a major improvement in both resolution (32 km, 3 h) and accuracy relative to the global NCEP/NCAR re-analysis (Mesinger *et al.*, 2006).

After computing T_E from T and q values using the method described in the previous section, we extracted monthly and seasonal subsets of the variables and derived their seasonal and monthly climatologies. Various calculations were performed on the gridded data, including: (1) mean absolute difference between T and T_E , differences between each of the variables at different levels (with significance assessed using the t -test); (2) the contribution of temperature and moisture to the magnitude of T_E (e.g. moisture contribution was computed as $(L_v q/H) \times 100$); (3) gridpoint correlations; (4) trend analysis and (5) additive decomposition of time series (Cleveland *et al.*, 1990; Makridakis *et al.*, 1998). The last consists of decomposing the time series into three components (trend + seasonality + random) and isolating the true trend signal.

Two types of trend calculations were made for both temperature and equivalent temperature: (1) simple linear trend estimates (linear least square regression) and corresponding p -values (at 0.05 and 0.01 significance levels) displayed in spatial distribution maps and (2) time series of linear trends using 10-year running windows, i.e. linear trends are computed for the first 10 years, and the window moves to the next 10 years at a monthly time step. As a result of this procedure which highlights long-term patterns, the trends time series were presented for the period December 1983 to January 1998. Trend calculations were performed on anomalies obtained from cosine-weighted spatially averaged time series.

The NDVI dataset from the Joint Institute for the Study of the Atmosphere and Ocean (JISAO, http://jisao.washington.edu/data_sets) was used to quantify the relationships between NDVI, T and T_E . NDVI is commonly used to investigate the effects of vegetation greenness and biomass density on near-surface energy partitioning and temperature (Sellers, 1985). It is derived from the radiance values of the visible (VIS) and near-infrared (NIR) channels: $NDVI = (NIR - VIS)/(NIR + VIS)$. Because of a number of limitations, NDVI, like other spectral vegetation indices, is not a perfect measure of vegetation biomass and greenness. However, it has the ability to distinguish vegetated areas from other land cover types and to survey vegetation dynamics. Analyses included: (1) correlation of the time series at a seasonal timescale using the Pearson product-moment method (Rodgers and Nicewander, 1988; Stigler, 1989); (2) gridpoint correlation of monthly T and T_E with NDVI and subsequent comparison of the spatial patterns; (3) assignment of gridpoint correlation values to each vegetation type using Geographic Information Systems (GIS) overlay techniques and summary statistics of the resulting correlation coefficients for each set and (4) for each gridpoint, calculation of the mean difference between T and T_E ; summary

statistics of the resulting difference values are computed for each land cover type.

For the gridpoint correlation, T and T_E were regridded to the coarser NDVI 1° increment. The monthly NDVI dataset spans the period July 1981 to September 2001 and as a result, T and T_E subsets were accordingly created. Over this study period, the monthly values of each T and T_E gridpoint have been correlated to the corresponding monthly values of NDVI to generate spatial patterns of correlation.

Two land cover datasets were used to relate both T and T_E to vegetation characteristics: (1) the classification derived from AVHRR (Hansen *et al.*, 2000) and (2) the National Land Cover Database (NLCD) 1992–2001 Retrofit Land Cover Change (Homer *et al.*, 2007). The AVHRR classification is a 1 km grid spacing data that originates from the Global Land Cover Facility (University of Maryland). It consists of 14 land cover types for North America (12 represented over the Continental United States, including the 9 vegetation classes used in this study); the dataset includes red, infrared and thermal bands in addition to the NDVI and has a length of record of 14 years (1981–1994), providing the ability to test the stability of classification algorithms (Hansen *et al.*, 2000). The NLCD dataset (30-m increment) consists of unchanged pixels between the two dates and changed pixels that are labelled with a 'from-to' land cover change value. In this study, only unchanged land cover types (9 classes out of 87) are considered, the remainder (78 change classes) being addressed in a subsequent study.

The GIS software ArcGIS (<http://www.esri.com>) was used to interpolate gridded surfaces of T and T_E values, and their correlation with NDVI. The data were linked to the land cover information using the Zonal Statistics method, which generates summary statistics of gridded surfaces values for each land cover type.

3. Results

3.1. Climatology

The monthly climatology of T , T_E and q at the 2-m level (1979–2005) is shown in Figure 1. T and T_E exhibit identical temporal patterns, but T_E values are larger. During the winter and early spring months with low humidity, differences between the two variables are small. As humidity increases from late spring to early fall, differences become much larger, especially during summer months (up to 22.74°C in July).

Overall, most of the magnitude of T_E is expressed by T , with q contributing a small proportion (Figure 2). The maximum contribution of moisture occurs during the summer months (11.01% in July). This distribution is consistent with the patterns shown in Figure 1.

Spatial patterns of the mean differences between T and T_E at various levels are displayed in Figure 3. At 2 m (and to a lesser extent at 850 mb), there is a sharp contrast between the eastern and western United States. Differences are larger in the Midwest and along the coastal Carolinas (up to 8°C) and decrease westward (below

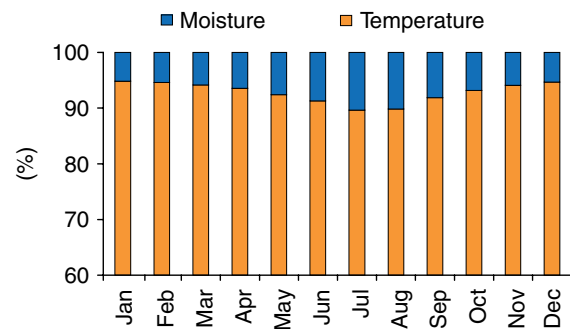


Figure 2. Monthly mean contribution of temperature and moisture (in %; level: 2 m) to the magnitude of equivalent temperature (1979–2005) over the United States. This figure is available in colour online at www.interscience.wiley.com/ijoc

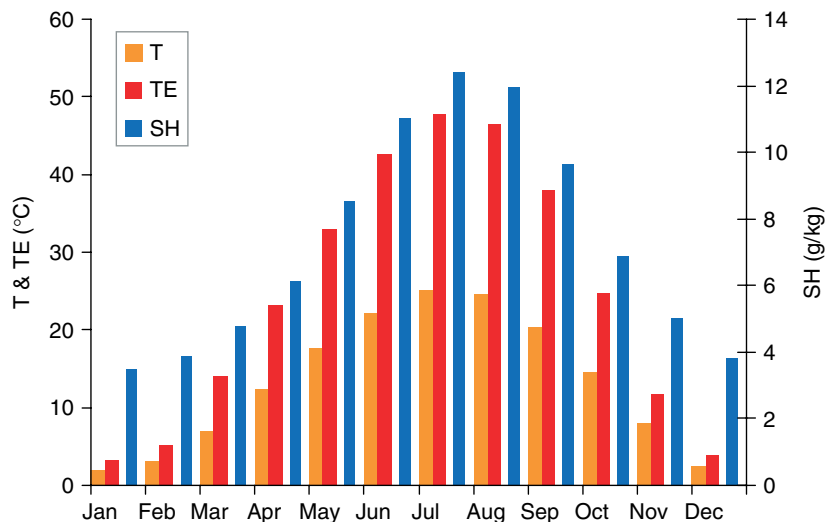


Figure 1. Monthly climatology of temperature (T), equivalent temperature (T_E) and specific humidity (SH) at 2 m (average 1979–2005) over the United States. The ordinate scale on the right pertains to values of specific humidity. This figure is available in colour online at www.interscience.wiley.com/ijoc

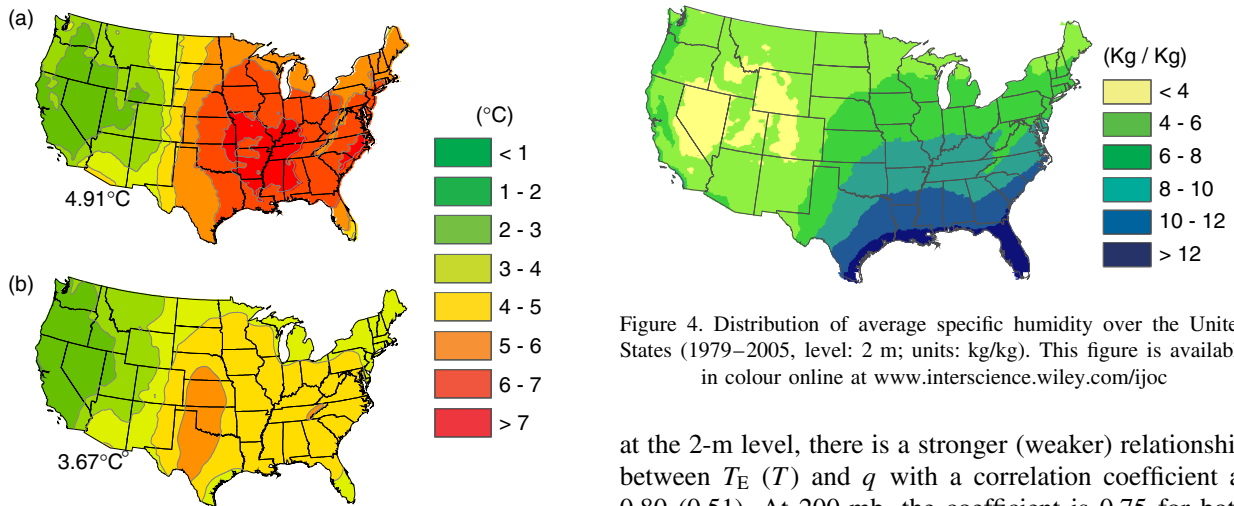


Figure 3. Mean absolute difference between T and T_E (1979–2005; units: $^{\circ}\text{C}$): (a) at 2 m and (b) at 850 mb. The averaged difference value is indicated. This figure is available in colour online at www.interscience.wiley.com/ijoc

2°C over the mountainous regions). These patterns are consistent with the temperature and moisture distribution: on average, q values are much larger in the eastern part of the country (Figure 4) and contribute to larger values of T_E . In contrast, both T and q are low over most of the Rockies and as a result, there are small differences between T and T_E . As shown in Figure 3, differences between T and T_E decrease with altitude (average difference of 4.91°C at 2 m, 3.67°C at 850 mb) and become small at 500 and 200 mb (0.63 and 0.02°C , respectively, not shown). This trend appears clearly in Figure 5, which shows the interannual variations of T , T_E and q . The time series depict a contrast between near-surface (2 m) and upper air T and T_E : the near-surface differences are statistically significant at 5% significance level, in contrast with the 200 mb level (not shown) which shows minor differences between T and T_E . The varying amount of q as a function of altitude is a key factor of the surface/upper-level contrast between T and T_E because nearly half the total water vapour in the air is found within the lowest 1.5 km layer (Ross *et al.*, 2002; Seidel, 2002).

T and T_E exhibit an increasing (decreasing) trend at 2 m (200 mb) and are both positively correlated with q :

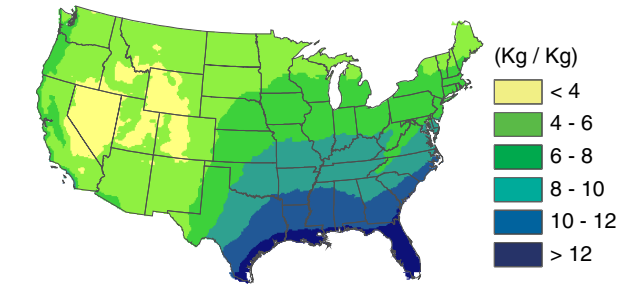


Figure 4. Distribution of average specific humidity over the United States (1979–2005, level: 2 m; units: kg/kg). This figure is available in colour online at www.interscience.wiley.com/ijoc

at the 2-m level, there is a stronger (weaker) relationship between T_E (T) and q with a correlation coefficient at 0.80 (0.51). At 200 mb, the coefficient is 0.75 for both T versus q and T_E versus q .

3.2. Trends

Decadal anomaly trends at different levels (Figure 6) indicate a statistically significant warming of both T and T_E , with values generally decreasing from near-surface (T , $0.31^{\circ}\text{C}/\text{decade}$; T_E , $0.52^{\circ}\text{C}/\text{decade}$) to 300 mb (T , $0.15^{\circ}\text{C}/\text{decade}$; T_E , $0.16^{\circ}\text{C}/\text{decade}$). At 200 mb, there is a decreasing trend for both variables ($-0.23^{\circ}\text{C}/\text{decade}$ for both T and T_E). This gradual decrease upward is disrupted at the 700 mb level, which records larger increase than the level below (850 mb) for both T and T_E . The reason for this pattern is not clear. As depicted in Figure 6, trend differences between T and T_E are larger at 2 m ($0.21^{\circ}\text{C}/\text{decade}$) and decrease upward. At 200 mb, there is very little trend difference ($0.003^{\circ}\text{C}/\text{decade}$). In summary, there is an increasing trend for both T and T_E up to 300 mb, with the largest increases observed near the surface. Above the 300-mb level, there is a decreasing trend for both variables.

The near-surface long-term trends (Figure 7(a)) show that T and T_E are closely related, with the exception of a period of abrupt decreasing trend in the early 1990s. During this period, T trends are much cooler than T_E trends. Temperature records worldwide experienced a decrease following the eruption of Mount Pinatubo on June 1991 (Parker *et al.*, 1996). However, at the same time, there is a substantial increase of q trends that helps

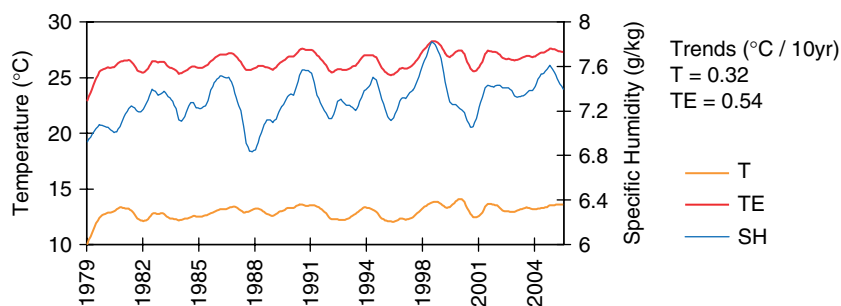


Figure 5. Time series for temperature (T), equivalent temperature (T_E) and specific humidity (SH) over the United States (level: 2 m). Seasonality and random variations have been removed (additive decomposition method). This figure is available in colour online at www.interscience.wiley.com/ijoc

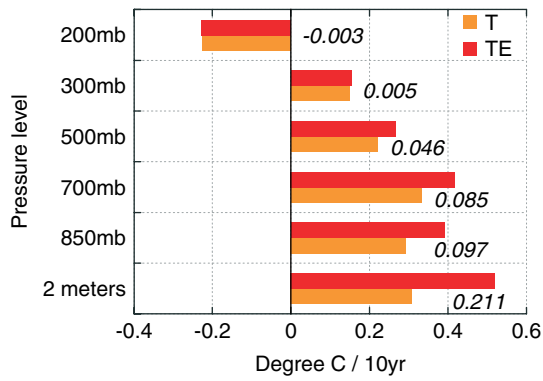


Figure 6. Decadal anomaly trends computed from monthly T and T_E at different pressure levels (1979–2005; units: $^{\circ}\text{C}/10$ years). Italicised values denote the differences T_E minus T . All trends are significant at the 5% level (p -value <0.05). This figure is available in colour online at www.interscience.wiley.com/ijoc

to maintain T_E trends at a much higher level than T trends [a positive trend in water vapour has been observed over the global oceans as well (Santer *et al.*, 2007)].

As a result, this period records the largest differences between the two variables (up to $0.67^{\circ}\text{C}/\text{decade}$ in the early 1990s). Overall, T_E shows more increase than T (a $0.9^{\circ}\text{C}/\text{decade}$ difference) over the study period. The long-term trends at 500 mb (Figure 7(b)) show the same patterns as the 2-m trends, although with less decrease. The 500 mb analysis confirms that the magnitude of the q trend contributes to the magnitude of differences between T and T_E trends: largest increases in q trends (e.g. early 1990s) correspond to the largest differences between T_E and T .

The 2-m seasonal anomaly trends (Table I) show that most of the increase for both T and T_E has occurred during winter ($0.71^{\circ}\text{C}/\text{decade}$ and $0.98^{\circ}\text{C}/\text{decade}$, respectively), whereas the trends reach their lowest values in summer (0.03 and $0.24^{\circ}\text{C}/\text{decade}$, respectively). Seasonal anomaly trends of q (not shown) follow the same temporal patterns: the increasing trend in q from spring to summer (0.0011 kg/kg/decade to 0.014 kg/kg/decade) compensates the summer decreasing T trend and helps maintain a larger T_E trend.

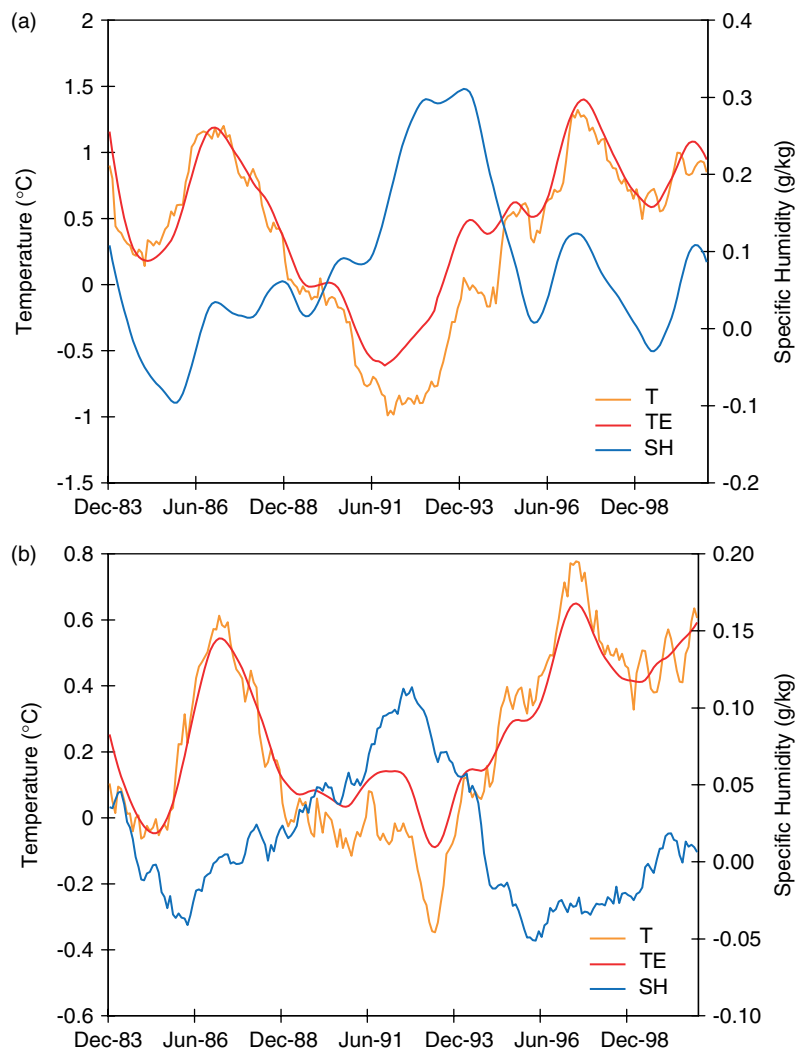


Figure 7. Trends of 10-year running window for temperature (T), equivalent temperature (T_E) and specific humidity (SH) anomalies (1979–2003). As a result of the running windows, the time series starts in December 1983, which represents the middle of the first 10-year window: (a) at 2 m, and (b) at 500 mb. This figure is available in colour online at www.interscience.wiley.com/ijoc

Table I. Seasonal anomaly trends for temperature and (equivalent temperature).

Level	DJF	MAM	JJA	SON
2 m	0.71 (0.98)	0.11 (0.30)	0.03 (0.24)	0.21 (0.45)
850 mb	0.59 (0.53)	0.13 (0.17)	0.09 (0.14)	0.26 (0.36)
700 mb	0.43 (0.53)	0.26 (0.31)	0.19 (0.32)	0.33 (0.47)
500 mb	0.27 (0.30)	0.17 (0.21)	0.10 (0.20)	0.31 (0.35)
300 mb	0.07 (0.07)	0.18 (0.05)	0.06 (0.06)	0.20 (0.20)
200 mb	-0.43 (-0.43)	-0.24 (-0.24)	-0.18 (-0.18)	-0.05 (-0.06)

Units are in $^{\circ}\text{C}/10$ years. Trend values in bold are significant at the 5% level.

From the 2-m level to 700 mb, the largest increases in both T and T_E occur during winter. Above 700 mb, most of the increase takes place in fall. At 200 mb, the strongest decrease takes place in winter (in contrast with the 2-m level) and there is no substantial difference between T and T_E trends for all seasons. This similarity between T and T_E at 300–200 mb is a consistent pattern.

Figure 8 shows the 2-m level geographical distribution of decadal T and T_E anomaly trends over the United States. Although the spatial patterns of T and T_E trends agree in that they both show areas of statistically significant increase over the eastern United States (around the Great Lakes and upper Midwest) and areas of decrease over the Rockies, T_E trends are much larger in magnitude ($0.45^{\circ}\text{C}/\text{decade}$ in average) and affect larger areas (e.g. over $1.2^{\circ}\text{C}/\text{decade}$ in southern Texas). The trends are significant at the 5% significance level over most of the eastern (both T and T_E) and southern United States (T only), and along the western coast (both T and T_E). Such distribution patterns suggest that there is a close relationship between T_E and q : areas where q trends increase significantly (not shown) tend to correspond to areas where T_E trends are large (e.g. southern Texas and eastern coast). But T also is a key-driver of T_E as shown by the similar distribution patterns of both variables over

the Midwest. At 200 mb (Figure 8(b)), the spatial patterns and magnitude of both T and T_E are almost identical (about $0.23^{\circ}\text{C}/\text{decade}$ in average). There is a generalised decrease for both variables, mainly over the central and northwestern United States. The trends are significant at the 5% level over the whole the United States, with the exception of spots over the northeast and southwest.

3.3. T and T_E in relation to vegetation properties

To investigate T and T_E with respect to vegetation properties at the 2-m level, we examine their time series correlation with NDVI and associate the resulting coefficients with vegetation types.

The land surface has been – and is still – experiencing various changes that alter its climate, both through surface reflectivity (albedo) and through the surface hydrologic cycle (Pielke *et al.*, 2002). Changes in surface moisture and energy fluxes trigger local and regional climate responses which can be of a similar magnitude to that projected for future greenhouse gas concentrations (Feddema *et al.*, 2005; Diffenbaugh 2005a, 2005b). For instance, vegetation affects the surface energy budget through transpiration (e.g. release of latent heat). Numerical studies have shown that using scenarios with different vegetation covers leads to significant climatic changes (e.g.

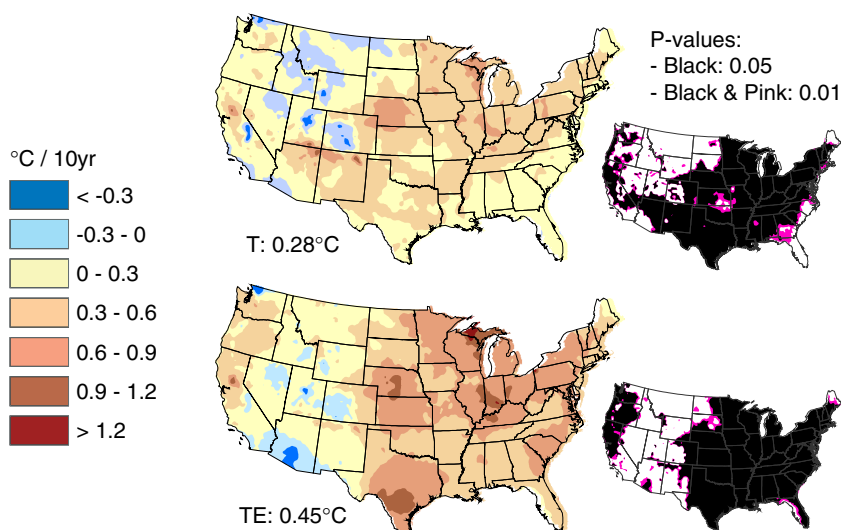


Figure 8. Temperature (T) and equivalent temperature (T_E) anomaly trends per decade computed from monthly data (period: 1979–2005; units: $^{\circ}\text{C}/10$ years). The average value of the trend is indicated for each variable. p -values are statistical significance levels 0.05 and 0.01. (a) Level: 2 m; (b) level: 200 mb. This figure is available in colour online at www.interscience.wiley.com/ijoc

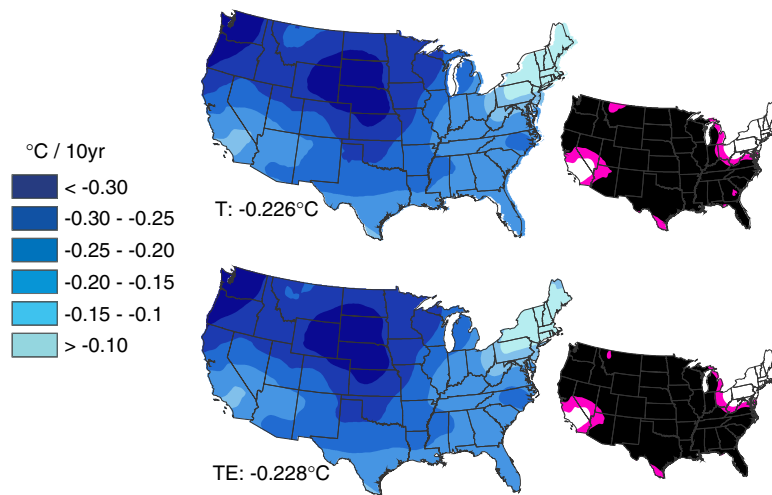


Figure 8. (Continued).

Bonan, 1997; Bounoua *et al.*, 2000). The relationships between NDVI and climate factors have been investigated in numerous studies (e.g. Townshend and Justice, 1986; Wang *et al.*, 2003; Sarkar and Kafatos, 2004; Carlson, 2008; Niyogi *et al.*, 2010).

The correlation of T and T_E with NDVI at a seasonal time scale (Figure 9) reveals that the highest correlations ($r > 0.72$) occur in winter with almost no differences between T and T_E . NDVI is less correlated with T and T_E during the spring season but the values remain relatively close (0.49 and 0.55, respectively). The lowest correlations with NDVI but largest differences between T and T_E are observed during the growing season: while T is negatively correlated with NDVI (-0.31), T_E exhibits a positive relationship (0.49). The differences are statistically significant at the 5% level. It is likely that increased biomass and vegetation transpiration play a role in these differences. The negative correlation between T and NDVI is consistent with findings that point to a cooling of T in the northern latitudes during the growing season, because of the seasonal increase in biomass and greenness and a reduced Bowen ratio (Bounoua *et al.*, 2000).

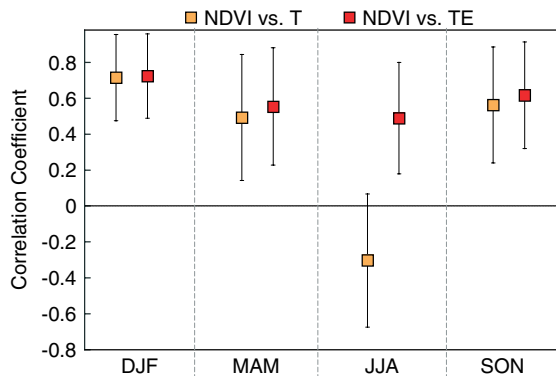


Figure 9. Pearson product-moment correlation of NDVI with T and T_E time series (level: 2 m) at seasonal time scale (1981–2001). Error bars denote 95% confidence intervals. This figure is available in colour online at www.interscience.wiley.com/ijoc

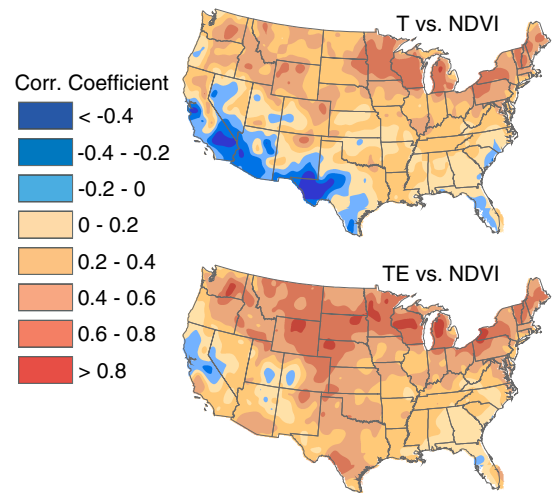


Figure 10. Gridpoint correlation of NDVI with T and T_E at (1981–2001; level: 2 m). All datasets were regridded at a common scale (1°) and for each gridpoint, monthly values over the study period were used for the correlation. This figure is available in colour online at www.interscience.wiley.com/ijoc

Distribution patterns of gridpoint correlation coefficients between NDVI and the two variables (T and T_E ; Figure 10) show a zonal contrast between relatively larger positive values over the northern United States (for both T and T_E) and a swath of negative correlation coefficients along the Mexican border and southern California (T only). Correlation coefficients averaged over the United States show that T_E is better correlated to NDVI than T (0.43 and 0.25, respectively).

The correlation between NDVI and T or T_E varies with vegetation type. It is worth acknowledging that our analysis summarises correlation coefficients for land cover types that extend over broad geographic areas, and the large-scale climate may vary within each or some of them. Therefore, averaging over land cover types may partly occult finer scale climatic variations.

Figure 11 shows correlation coefficients for NDVI versus T and NDVI versus T_E averaged as a function of

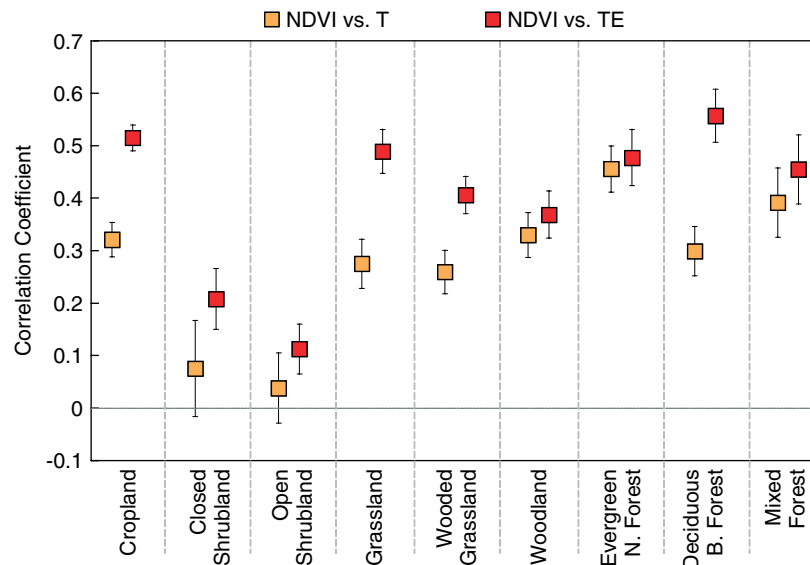


Figure 11. Mean correlation coefficient of NDVI *versus* T and T_E (level: 2 m) as a function of vegetation type. Mean correlation values and confidence interval were obtained using the ArcGIS Zonal Statistics method, which computes from a gridded dataset summary statistics for each zone (here, vegetation types). Error bars denote 95% confidence intervals at 5%. This figure is available in colour online at www.interscience.wiley.com/ijoc

vegetation types derived from AVHRR land cover classification. NDVI and T_E are more correlated over deciduous broadleaf forests, croplands and grasslands (0.56, 0.52 and 0.49 respectively). This stronger T_E –NDVI relationship may be in part explained by increased vegetation greenness (especially during the growing season) which, of course, is associated with larger transpiration. This relationship is consistent with the summer patterns displayed in Figure 9. While most of near-surface moisture over agricultural land is because of transpiration and/or the physical evaporation from irrigated areas, deciduous broadleaf forests are characterised by a high evaporative fraction because of a relatively high leaf area index (Baldocchi, 2005; Bonan, 2008). The largest correlations between NDVI and T are found in evergreen needleleaf forests, mixed forests and woodlands (0.46, 0.39 and 0.33, respectively). Over drier areas (e.g. shrublands), NDVI is weakly correlated with both T and T_E . The

differences between T and T_E are statistically significant (5% significance level) over croplands, deciduous broadleaf forests and grasslands. Moreover, over these vegetation types with relatively high transpiration rates, NDVI *versus* T_E exhibits smaller standard deviations (e.g. 0.15 and 0.19 over croplands and deciduous broadleaf forests) than NDVI *versus* T (0.32 and 0.25, respectively), indicating that the correlation coefficients for T_E did not vary much and remained relatively high. Apart from one notable exception for which NDVI *versus* T displays a smaller value (evergreen needleleaf forest), the larger standard deviations for NDVI *versus* T suggest that the relationships between NDVI and T are less pronounced than the ones with T_E .

The mean differences between T_E and T as a function of land cover types that did not change between 1992 and 2001 (Figure 12) show a contrast between moist and drier areas. The largest differences are found

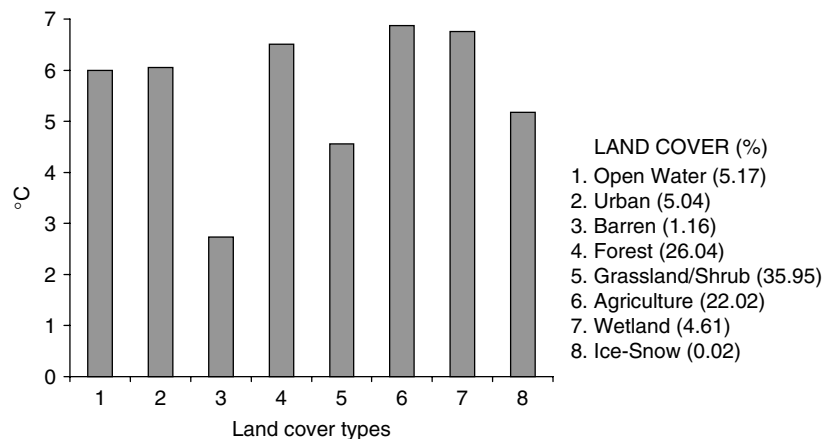


Figure 12. Mean difference between T_E and T as a function of NLCD land cover types that did not change between 1992 and 2001 (units: °C). Mean difference values for each gridpoint are used to compute statistics for each land cover type.

in croplands (6.9°C), wetlands (6.7°C), forests (6.5°C), urban areas (6.05°C) and open water (6°C). Barren areas and grasslands/shrublands exhibit the lowest differences (2.7°C and 4.5°C respectively). The most statistically reliable differences (with the smallest confidence intervals at the 5% significance level) are found in larger samples: grasslands/shrublands (36% of land cover areas that did not change), forests (26%) and croplands (24%). These results suggest that various land cover types influence moisture availability in the lower atmosphere and that T_E is larger in areas with higher physical evaporation and transpiration rates. Betts *et al.* (1996) and Holt *et al.* (2006) demonstrated that local-scale moisture fluxes into the atmosphere can significantly impact the atmospheric thermodynamic structure, modify boundary layer settings and contribute to heavy rainfall, and that short- and medium-range forecasts produce much better predictions when such factors are included in land surface parameterisation.

4. Conclusions

The T_E is strongly driven by T , which accounts for about 90% of its magnitude. This can be seen in various time-series in which both T and T_E exhibit similar fluctuation patterns. However, despite its small contribution to the magnitude of T_E , the moisture component induces larger trends of T_E relative to T . The differences between the two variables can be explained by the fact that the moisture component of T_E is strongly influenced by atmospheric near-surface moisture (e.g. from vegetation transpiration and soil moisture evaporation). Indeed, our analysis has shown that at the 2-m level, there is a stronger relationship between T_E and q ($r = 0.8$) than T and q ($r = 0.51$), but this large difference decreases upward and disappears at 300–200 mb. In contrast to pronounced temporal and spatial differences at the near-surface levels, this similarity between T and T_E at 300–200 mb is a consistent pattern: (1) the differences between the two variables averaged over the study period are large at the 2-m level but very small at 200 mb; (2) T and T_E time series present statistically significant differences at the 2-m level but minor differences at 200 mb; (3) the decadal anomaly trend differences are large at the 2-m level (up to 0.21°C/decade) but very small at 200 mb (–0.003°C/decade).

Our results suggest that land cover types influence both moisture availability and temperature in the lower atmosphere, and that T_E is larger in areas with higher evaporation and transpiration rates. During summer, T_E exhibits positive (though relatively moderate) correlation with NDVI, while T –NDVI correlation remains negative. This relationship suggests that T_E is more correlated to biomass increase, vegetation transpiration and other surface moisture characteristics. Moreover, correlation coefficients averaged over the United States depict a stronger relationship between T_E and NDVI, especially over vegetation types that are characterised by a

high transpiration rate (e.g. deciduous broadleaf forests and croplands). Using T_E to assess tropospheric heating trends is not only an efficient way to investigate the vertical structure of the combined effects of temperature and moisture, but it may also help obtain an improved estimate of the impacts of surface properties on heating trends.

Although the calculation of T_E has been performed by combining sensible ($C_p T$) heat and moisture ($L_v q$), the emphasis in terms of moisture has been put on q only. For a better diagnosis of T_E , subsequent studies should additionally focus on: (1) the surface energy budget, as soil moisture and other flux measurements combined with q can help to better explain the magnitude and variability of T_E at 2 m; (2) the effects of atmospheric circulation on the variability of q and resulting T_E and (3) fingerprint studies that aim to determine the contribution of anthropogenic influences on T_E magnitude and variability (e.g. Santer *et al.*, 2007).

Acknowledgements

We thank Alan K. Betts for providing supporting documents. We would also like to thank Dallas Staley for her outstanding contribution in editing and finalising the paper, and Dr Kapo Coulibali for providing R scripts. The study benefited from the DOE ARM Program (08ER64674; Dr Rick Petty and Dr Kiran Alapaty), and in parts from NASA Terrestrial Hydrology Program (Dr Jared Entin), and NSF CAREER-0847472 (Liming Zhou and Jay Fein). R. A. Pielke Sr. received support to complete this study from the University of Colorado at Boulder (CIRES/ATOC).

References

- Baldocchi DD. 2005. The role of biodiversity on the evaporation of forests. In *Forest Diversity and Function: Temperate and Boreal Systems, Ecological Studies 176*, Scherer-Lorenzen M, Schulze ED (eds). Springer-Verlag: Berlin; 131–148.
- Barnett TP, Adam JC, Lettenmaier DP. 2005b. Potential impacts of a warming climate on water availability in snow-dominated regions. *Nature* **438**: 303–309.
- Barnett TP, Pierce DW, AchutaRao KM, Gleckler PJ, Santer BD, Gregory JM, Washington WM. 2005a. Penetration of human-induced warming into the world's oceans. *Science* **309**: 284–287.
- Betts AK, Ball JH, Beljaars ACM, Miller MJ, Viterbo P. 1996. The land surface atmosphere interaction: a review based on observational and global modeling perspectives. *Journal of Geophysical Research* **101**: 7209–7225.
- Bonan GB. 1997. Effects of land use on the climate of the United States. *Climatic Change* **37**: 449–486.
- Bonan GB. 2008. Forests and climate change: forcings, feedbacks and the climate benefits of forests. *Science* **320**: 1444–1449.
- Bounoua L, Collatz GJ, Los S, Sellers PJ, Dazlich DA, Tucker CJ, Randall DA. 2000. Sensitivity of climate to changes in NDVI. *Journal of Climate* **13**: 2277–2292.
- Cleveland RB, Cleveland WS, Mcrae JE, Terpenning I. 1990. STL: a seasonal-trend decomposition procedure based on Loess. *Journal of Official Statistics* **6**(1): 3–73.
- Carlson T. 2008. An overview of the “Triangle Method” for estimating surface evapotranspiration and soil moisture from satellite imagery. *Sensors* **7**: 1612–1629.
- Crowley TJ, Lowery T. 2000. How warm was the medieval warm period? *Ambio* **29**: 51–54.
- Davey CA, Pielke RA Sr, Gallo KP. 2006. Differences between near-surface equivalent temperature and temperature trends for the eastern

- United States: equivalent temperature as an alternative measure of heat content. *Global and Planetary Change* **54**: 19–32.
- Diffenbaugh NS. 2005a. Atmosphere-land cover feedbacks alter the response of surface temperature to CO₂ forcing in the western United States. *Climate Dynamics* **24**: 237–251, DOI: 10.1007/s00382-004-0503-0.
- Diffenbaugh NS. 2005b. Sensitivity of extreme climate events to CO₂-induced biophysical atmosphere-vegetation feedbacks in the western United States. *Geophysical Research Letters* **32**: L07702, DOI: 10.1029/2004GL022184.
- Feddema JJ, Oleson KW, Bonan GB, Mearns LO, Buja LE, Meehl GA, Washington WM. 2005. The importance of land-cover change in simulating future climates. *Science* **310**: 1674–1678.
- Gaffen DJ, Ross RJ. 1999. Climatology and trends in U.S. surface humidity and temperature. *Journal of Climate* **12**: 811–828.
- Hansen M, DeFries R, Townshend JRG, Sohlberg R. 2000. Global lands cover classification at 1 km resolution using a decision tree classifier. *International Journal of Remote Sensing* **21**: 1331–1365.
- Held IM, Soden BJ. 2006. Robust responses of the hydrological cycle to global warming. *Journal of Climate* **19**(21): 5686–5699.
- Holt T, Niyogi D, Chen F, LeMone MA, Manning K, Qureshi AL. 2006. Effect of land-atmosphere interactions on the IHOP 24–25 May 2002 convection case. *Monthly Weather Review* **134**: 113–133.
- Homer C, Dewitz J, Fry J, Coan M, Hossain N, Larson C, Herold N, McKerrow A, VanDriel JN, Wickham J. 2007. Completion of the 2001 National Land Cover database for the conterminous United States. *Photogrammetric Engineering and Remote Sensing* **73**(4): 337–341.
- Intergovernmental Panel on Climate Change (IPCC). 2001. *Climate Change 2001: The Scientific Basis*. Contribution of Working Group I to the Third Assessment Report of the Intergovernmental Panel on Climate Change. Houghton JT, Ding Y, Griggs DJ, Noguer M, van der Linden PJ and Xiaosu D (eds). Cambridge University Press: Cambridge, New York.
- Intergovernmental Panel on Climate Change (IPCC). 2007. Summary for policymakers. In *Climate Change 2007: The Physical Science Basis*. Contribution of Working Group I to the Fourth Assessment Report of the Intergovernmental Panel on Climate Change. Solomon S, Qin D, Manning M, Chen Z, Marquis M, Averyt KB, Tignor M and Miller HL, (eds). Cambridge University Press: Cambridge, New York.
- Jones PD, Raper SCB, Bradley RS, Diaz HF, Kelly PM, Wigley TML. 1986. Northern Hemisphere surface air temperature variations: 1851–1984. *Journal of Climate and Applied Meteorology* **25**(2): 161–179.
- Makridakis S, Wheelwright SC, Hyndman RJ. 1998. *Forecasting Methods and Applications*, 3rd edn. John Wiley & Sons: New York.
- Mann ME, Jones PD. 2003. Global surface temperatures over the past two millennia. *Geophysical Research Letters* **30**(15): 1–4.
- Mears CA, Wentz FJ. 2005. The effect of diurnal correction on satellite-derived lower tropospheric temperature. *Science* **309**: 1548–1551.
- Mesinger F, DiMego G, Kalnay E, Mitchell K, Shafran PC, Ebisuzaki W, Jovic D, Woollen J, Rogers E, Berbery EH, Ek MB, Fan Y, Grumbine R, Higgins W, Li H, Lin Y, Manikin G, Parrish D, Shi W. 2006. North American Regional Reanalysis: a long-term, consistent, high-resolution climate dataset for the North American domain, as a major improvement upon the earlier global reanalysis datasets in both resolution and accuracy. *Bulletin of the American Meteorological Society* **87**: 343–360.
- Moberg A, Sonechkin DM, Holmgren K, Datsenko NM, Karlen W. 2005. Highly variable Northern Hemisphere temperatures reconstructed from low- and high-resolution proxy data. *Nature* **433**: 613–618.
- Niyogi D, Kishtawal CM, Tripathi S, Govindaraju RS. 2010. Observational evidence that agricultural intensification and land use change is reducing the Indian summer monsoon rainfall. *Water Resources Research* (in press).
- Parker DE, Wilson, H Jones PD, Christy JR, Folland CK. 1996. The impact of Mount Pinatubo on worldwide temperatures. *International Journal of Climatology* **16**: 487–497.
- Pielke RA Sr. 2003. Heat storage within the Earth system. *Bulletin of the American Meteorological Society* **84**: 331–335.
- Pielke RA Sr, Davey C, Morgan J. 2004. Assessing “global warming” with surface heat content. *Eos Transactions* **85**(21): 210–211.
- Pielke RA Sr, Marland G, Betts RA, Chase TN, Eastman JL, Niles JO, Niyogi D, Running S. 2002. The influence of land-use change and landscape dynamics on the climate system: relevance to climate change policy beyond the radiative effect of greenhouse gases. *Philosophical Transactions of the Royal Society London A* **360**: 1705–1719.
- Ribera P, Gallego D, Gimeno L, Pérez JF, García R, Hernández E, de la Torre L, Nieto R, Calvo N. 2004. The use of equivalent temperature to analyze climate variability. *Studia Geophysica et Geodaetica* **48**: 459–468.
- Rodgers JL, Nicewander WA. 1988. Thirteen ways to look at the correlation coefficient. *The American Statistician* **42**(1): 59–66.
- Ross RJ, Elliott WP, Seidel DJ, Participating AMIP-II Modeling Groups. 2002. Lower-Tropospheric humidity – temperature relationships in radiosonde observations and atmospheric general circulation models. *Journal of Hydrometeorology* **3**: 26–38.
- Santer BD, Mears C, Wentz FJ, Taylor KE, Gleckler PJ, Wigley TML, Barnett TP, Boyle JS, Brueggemann W, Gillett NP, Klein SA, Meehl GA, Nozawa T, Pierce DW, Stott PA, Washington WM, Wehner MF. 2007. Identification of human-induced changes in atmospheric moisture content. *Proceedings of the National Academy of Sciences* **104**: 15248–15253, DOI: 10.1073/pnas.0702872104.
- Santer BD, Thorne PW, Haimberger L, Taylor LKE, Wigley TML, Lanzante JR, Solomon S, Free M, Gleckler PJ, Jones PD, Karl TR, Klein SA, Mears C, Nychka D, Schmidt GA, Sherwood SC, Wentz FJ. 2008. Consistency of modelled and observed temperature trends in the tropical troposphere. *International Journal of Climatology* **28**: 1703–1722.
- Santer BD, Wigley TML, Mears C, Wentz FJ, Klein SA, Seidel DJ, Taylor KE, Thorne PW, Wehner MF, Gleckler PJ, Boyle JS, Collins WD, Dixon KW, Doutriaux C, Free M, Fu Q, Hansen JE, Jones GS, Ruedy R, Karl TR, Lanzante JR, Meehl GA, Ramaswamy V, Russell G, Schmidt GA. 2005. Amplification of surface temperature trends and variability in the tropical atmosphere. *Science* **309**: 1551–1556.
- Sarkar S, Kafatos M. 2004. Interannual variability of vegetation over the Indian subcontinent and its relation to the different meteorological parameters. *Remote Sensing of the Environment* **90**: 268–280.
- Seidel DJ. 2002. *Water Vapor: Distribution and Trends, Encyclopedia of Global Environmental Change*. John Wiley & Sons: Chichester, UK.
- Sellers PJ. 1985. Canopy reflectance, photosynthesis, and transpiration. *International Journal of Remote Sensing* **6**: 1335–1372.
- Sherwood SC, Lanzante JR, Meyer CL. 2005. Radiosonde daytime biases and late 20th century warming. *Science* **309**: 1556–1559.
- Soon W-H, Legates DR, Baliunas S. 2004. Estimation and representation of long-term (>40 year) trends of Northern Hemisphere-gridded surface temperature: a note of caution. *Geophysical Research Letters* **31**: L03209, DOI: 1029/2003GRL019141.
- Steadman RG. 1979. The assessment of sultriness, part 2: effects of wind, extra radiation and barometric pressure on apparent temperature. *Journal of Applied Meteorology* **18**: 874–885.
- Steadman RG. 1984. A universal scale of apparent temperature. *Journal of Applied Meteorology and Climatology* **23**: 1674–1687.
- Stigler SM. 1989. Francis Galton’s account of the invention of correlation. *Statistical Science* **4**(2): 73–79.
- Townshend JRG, Justice CO. 1986. Analysis of the dynamics of African vegetation using the normalized difference vegetation index. *International Journal of Remote Sensing* **7**: 1435–1446.
- Vinnikov KY, Groisman PY, Luginina KM. 1990. Empirical data on contemporary global climate changes (temperature and precipitation). *Journal of Climate* **3**: 662–677.
- Wang J, Rich PM, Price KP. 2003. Temporal response of NDVI to precipitation and temperature in the central Great Plains. *International Journal of Remote Sensing* **24**: 2345–2364.
- Wentz FJ, Ricciardulli L, Hilburn K, Mears C. 2007. How much more rain will global warming bring? *Science* **317**: 233–235.
- Wentz FJ, Schabel MC. 2000. Precise climate monitoring using complementary satellite data sets. *Nature* **403**: 414–416.